World Applied Sciences Journal 21(Special Issue of Engineering and Technology): 60-67, 2013
ISSN 1818-4952

DOI: 10.5829/idosi.wasj.2013.21.1008

Optical and Mott-Schottky Studies of Ternary MoSSe Thin Films Synthesized by Electrochemical Route

[1]T. Joseph Sahaya Anand, [1]S. Shariza, [1]Z.M. Rosli, [1]A. Shaaban, [2]Sivarao, [3]Said, Mohamad Radzai, [4]Kamaruzaman Jusoff and [5]S. Thiru

[1]Department of Engineering Materials,
[2]Department of Manufacturing Process, Faculty of Manufacturing Engineering,
[3]Department of Structure and Materials, Faculty of Mechanical Engineering,
Universiti Teknikal Malaysia Melaka (UTeM), Hang Tuah Jaya,
76100 Durian Tunggal, Melaka, Malaysia
[4]Department of Forest Production, Faculty of Forestry,
Universiti Putra Malaysia, 43400 UPM, Serdang, Selangor, Malaysia
[5]Department of Design and Innovation, Faculty of Mechanical Engineering,
Universiti Teknikal Malaysia Melaka (UTeM), Hang Tuah Jaya,
76100 Durian Tunggal, Melaka, Malaysia

Abstract: The objectives of this paper is to synthesise the ternary molybdenum sulphoselenide MoSSe thin films via electrodeposition technique and analyse the effect of film thickness to its optical and semiconducting properties. Transition metal molybdenum sulphoselenide, MoSSe thin films have been electrosynthesized on indium-tin-oxide (ITO)-coated glass and stainless steel substrates. The thin films were characterized for their structural, surface morphological, compositional characteristics as well as optical properties and semiconducting parameters. Structural analysis via X-ray diffraction (XRD) reveals that the films are polycrystalline in nature. Scanning electron microscope (SEM) studies reveal the morphology of the film with crystallites on the surface. Compositional analysis via energy dispersive X-ray (EDX) analysis confirms the presence of Mo, S and Se elements in the films. The optical studies show that the films are of direct bandgap. Results on the semiconductor parameters analysis of the films showed that the nature of the Mott-Schottky plots indicates that the films obtained are of n-type material. For all films, the semiconductor parameter values come in the potential range of leading chalcogenides as a semiconductor thin film which can be suitable for photo electrochemical solar cell in the near future.

Key words: Molybdenum Sulphoselenide % Electrodeposition % Scanning Electron Microscope (SEM) % Direct Bandgap % Mott-Schottky Plots

INTRODUCTION

Semiconductor materials are being actively investigated for direct conversion of light energy into electrical energy. The best materials for light energy conversion applications are narrow bandgap semiconductors in bulk or thin film form. Recently there has been a growing interest in layered semiconducting compounds consisting of group VIA transition metal dichalcogenides MX_2 (M = Mo, W and X = S, Se & Te) [1-3]. These potential materials for light energy conversion applications have stimulated interest in its basic properties. Binary transition metal chalcogenides thin films have already been elaborated by selenization [2], sputtered [4-5], solid state mechanism [6], sulfurization [7] and reduction by electrolytic [8].

These techniques are present special problems for the preparation of transition metal chalcogenide films and are relatively cost intensive [9]. However, limited amount of work has been carried out only on the other properties

Corresponding Author: T. Joseph Sahaya Anand, Department of Engineering Materials,
Faculty of Manufacturing Engineering, Universiti Teknikal Malaysia Melaka (UteM),
Hang Tuah Jaya, 76100 Durian Tunggal, Malaysia. Tel: +606-3316489, E-mail: anand@utem.edu.my

of electrodeposited ternary molybdenum MoSSe thin films. The cyclic voltammetry (CV) technique was used to derive the deposition potential of the chalcogenide thin film. With the utilization of electrodeposition technique, this research aims to design and predict a safe, non-toxic, cost-efficient and relatively simple method for synthesis of ternary transition metal chalcogenide thin films. The synthesis of ternary molybdenum sulphoselenide MoSSe thin films via electrodeposition technique and the effect of film thickness to its optical and semiconducting properties are conducted.

MATERIALS AND METHODS

Sample Preparation: Indium-tin-oxide (ITO)-coated glass and stainless steel substrates were cut into 15 × 25 mm size for the film deposition. ITO glass were dipped for few seconds into 50% diluted hydrochloric acid, HCl, rinsed with double distilled water then cleaned in hot air. Stainless steel substrates were mirror polished by polish (sand) paper and finally cleaned in an ultrasonic cleaner. This treatment increases the adhesion of the electrodeposits to the substrate and allows the thicker deposition without peeling. The precursors' molybdic acid (H_2MoO_4), sodium thiosulphate pentahydrate ($Na_2S_2O_3.5H_2O$) and selenium dioxide (SeO_2) were used respectively as Mo^{4+}, S^{2-} and Se^{2-} ion sources. To prepare electrolyte solutions H_2MoO_4 $Na_2S_2O_3.5H_2O$ and SeO_2 having concentration of 0.5M, there are three different solutions were first prepared: solution A containing H_2MoO_4 within ammonia, $Na_2S_2O_3.5H_2O$ are included in solution B and solution C has SeO_2 in distilled water. These solutions in proportional amounts were mixed as the precursor electrolyte.

Thin Films Synthesis via Electrodeposition: The Potentiostat by Princeton Applied Research Model VersaSTAT 3 Potentiostat was employed for the electrodeposition of transition metal ternary MoSSe thin films. The cyclic voltammetry (CV) technique was used to derive the deposition potential of the chalcogenide thin film continued by synthesis of the chalcogenides by electrodeposition technique. The CV measurement and electrodeposition of the film was adopted with a three - electrode cell system in a manner described by [10]. The setup of the system is shown in Figure 1. In the case for transition metal chalcogenide compounds the potential limit range -1.00 *V* to 1.00 *V* was found to be suitable [11-12] for the CV measurements.

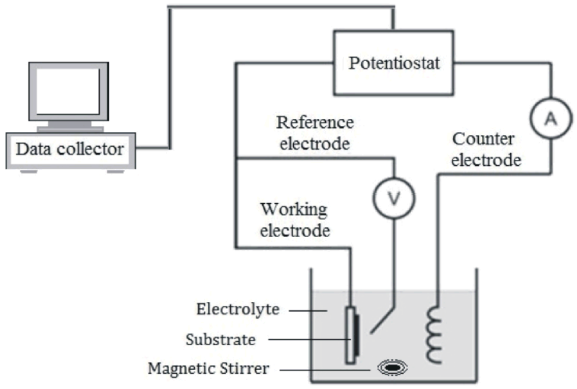

Fig. 1: Cell setup for electrodeposition of molybdenum sulphoselenide thin film

Characterization of Electrodeposited Thin Films: Film thickness of MoSSe was determined by gravimetric weight difference method using a sensitive microbalance and assuming film density as the bulk density of the compounds (6.04 g/cm^3 for MoSSe) [13] and the area of the film is . 2.25 cm^2. X-ray diffraction (XRD) and scanning electron microscopy (SEM) analysis were performed by using PANalytical ZPERT PROMPD PW 3040/60 diffractometer (for 2θ range from 20 to 60° with CuK_α radiation) and SEM ZEIZZ EVO 50 scanning microscope respectively and its composition analysis with energy dispersive X-ray (EDX) analysis. Optical properties and semiconductor parameters measurements of the films were carried out using UV-VIS spectrophotometer [10] and Mott-Schottky plot analysis [1] respectively.

RESULTS AND DISCUSSION

Electrochemistry of Mo, S and Se Systems: Thin film formation of MoSSe occurs as a result of the various chemical reactions taking place in the deposition bath. In the present investigation ionic species of molybdenum, sulphide and selenide are produced by the following reaction equilibria in an aqueous alkaline deposition bath.

$$H_2MoO_4 + 6H^+ + 2e^- \rightarrow Mo^{4+} + 4H_2O \quad (1)$$

$$HseO_2 + H_2O \rightarrow H_2SeO_3$$

On the Substrate Surface, H_2Seo_3 Reduces to Selenium:

$$H_2SeO_3 + 4H^+ + 6e^- \rightarrow Se^{2-} + 3H_2O \quad Na_2S_2O_3 : Na^{2+} + S_2O_3^{2-} \quad (2)$$

$$S_2O_3^{2-} + 6H^+ + 6e^- : 2S^{2-} + 3H_2O \quad (3)$$

Reaction (1) shows that metal ions are produced by dissociation of the metal complex while chalcogenide ions (Reactions (2) and (3)) are produced by dissociation of sulphur and selenium precursors in the aqueous alkaline medium. When the concentration of ionic species Mo^{4+}, S^{2-} and Se^{2-} exceeds in the reaction bath, nucleation starts which results in the growth of molybdenum sulphoselenide, MoSSe thin films. The following chemical reaction shows the yielding of insoluble molybdenum sulphoselenide thin film on substrate support:

$$Mo^{4+} + S^{2-} + Se^{2-} \rightarrow \text{MoSSe molybdenum sulphoselenide} \quad (4)$$

The cyclic voltammogram of the electrodes in ammoniacal $H_2MoO_4 + Na_2S_2O_3.5H_2O + SeO_2$ solution is shown in Figure 2. Cathodic current onset could be seen arising at -0.58*V* followed by a steady increase during the forward scan. This point marks the reduction process of ionic species to form MoSSe compound. The low current rise in the cathodic region indicates that hydrogen evolution occurs at a minimal rate. During the reverse scan, the dissolution of molybdenum sulphoselenide compound starts at approximately 0.7 *V*, confirmed by the oxidation peak in the anodic region.

Film Growth and Film Thickness: The growth of the films was studied through the film thickness plot as shown in Figure 3. Very thin film formation is observed for the first 10 minutes due the initial induction period. Thereafter, the film growth begins to form more uniformly on the substrate.

The initial induction period presence can be attributed to the growth mechanism as the nucleation occurs first before the combination of ions for the film growth [14]. The presence of this period is the evidence of a typical 'ion-by-ion' growth mechanism. The average deposition rate measured at deposition time less than 10 minutes is approximately 85 nm/min higher than that above 10 minutes, at approximately 20 nm/min. At the initial stage of the deposition, the average deposition rate is higher due to the high concentration of ions in the electrolyte and large substrate space for deposition. For any type of deposition, the rate of deposition will decrease then stop. In short, deposition cannot continue on the substrate anymore due to closely packed structure of the film on the substrate and ions deficiency in the electrolyte. All films obtained were well adherent to the substrates and uniform to the naked eye. The colour of MoSSe films were dark grey to black in colour.

Structural, Morphological and Compositional Characterization: The structural characterization by X-ray diffraction (XRD) measurement is a diffractogram, showing phases present (peak positions), phase concentrations (peak heights), amorphous content (background hump) and crystallite size / strain (peak widths) [15]. XRD patterns of MoSSe films deposited on stainless steel substrates at different deposition times are shown in Figure 4.

The polycrystalline planes of the crystals, indicated by sharp peaks are identified as (1 2 -4) and (1 4 0) planes of MoSSe and (1 1 1) and (2 2 0) planes of the substrate that used - stainless steel [16]. It is identified as rhombohedral structure of the MoSSe films and the structural features fit with lattice parameter values a = b = 0.9533 nm and c = 1.7363 nm which is in good agreement with the standard values [13]. The corresponding interplanar distances are in good agreement with the JCPDS data [13, 16] are summarized in Table 1.

There is only one peak identified as MoSSe peak at 2 =50.6° for the films deposited at a shorter period of time while the peaks for the stainless steel substrate are more visible. At 20 minutes deposition time, a MoSSe peak at 2 =44.49° starts to emerge and becomes more distinct from the neighbouring peak, indicating that the preferred orientation (1 2 -4) grains can be found only in thicker films. Observation shows (1 4 0) plane structure of MoSSe at 2 =50.62° and (22 0) plane structure of stainless steel at 2 =74.70° appear as constant peaks throughout. According to the Debye-Scherrer approach [17], from the X-ray diffractograms of the crystals corresponding to different (*h k l*) planes the estimated grain size were calculated and the values are in the range of 44 - 55 nm.

The surface morphology of MoSSe films deposited on stainless steel substrates at different deposition time is shown in Figure 5.

At longer deposition times, the structure of the films starts to break into grains (flakes) while still adhering to the substrate [18]. The grains of the materials keeps on growing with time, causing the films to break and forming flake-like structures upon reaching the maximum grain stress point. The cracking of the structure is also due to the drying shrinkage phenomena known to occur in

Table 1: XRD data Comparison of 'd' values for the ternary MoSSe thin film

			Experimental *'d'* value (Å)				
Angle (2θ)	(h k l)	STD (Å) $'d'_{JCPDS}$	10 min	15 min	20 min	25 min	30 min
43.582	(1 1 1)	2.0750	2.0919	2.0801	2.0744	2.0753	2.0755
44.487	(1 2 -4)	2.0348	-	-	2.0365	2.0339	2.0347
50.618	(1 4 0)	1.8015	1.8097	1.8022	1.8009	1.8007	1.7994
74.704	(2 2 0)	1.2697	1.2700	1.2723	1.2712	1.2713	1.2713

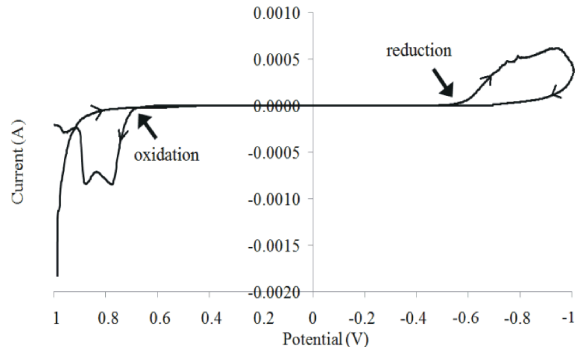

Fig. 2: Cyclic voltammogram of the electrodes H_2MoO_4 + $Na_2S_2O_3.5H_2O$ + SeO_2 in ammoniacal solution.

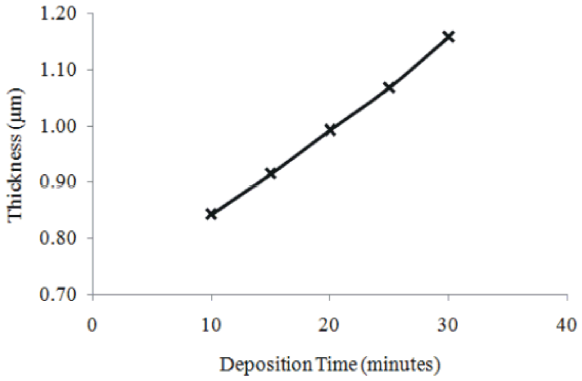

Fig. 3: Variation of thickness with deposition time for MoSSe films.

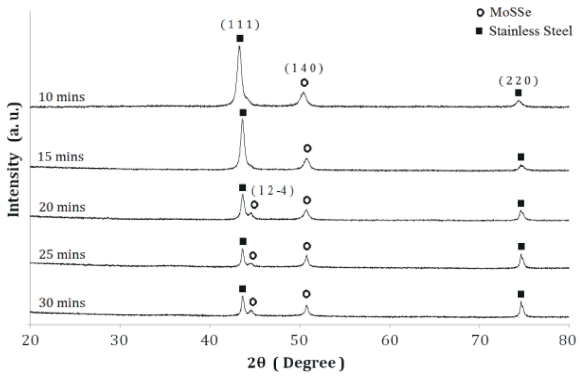

Fig. 4: XRD pattern for MoSSe thin films deposited at different deposition times

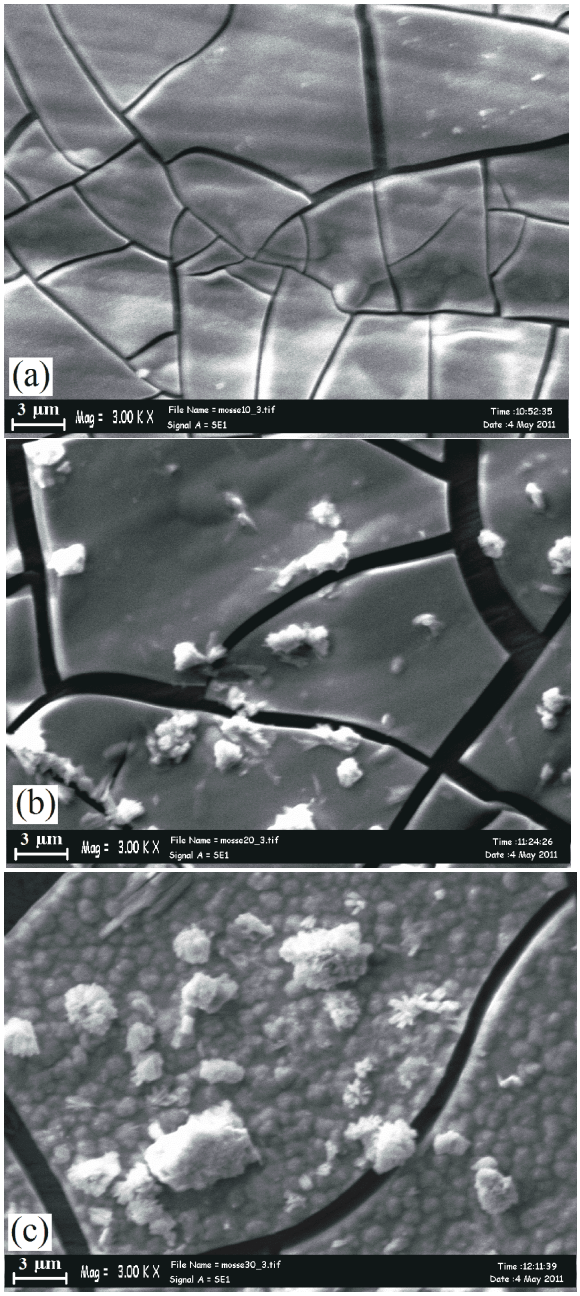

Fig. 5: SEM images of MoSSe films deposited for (a) 10 min, (b) 20 min and (c) 30 min.

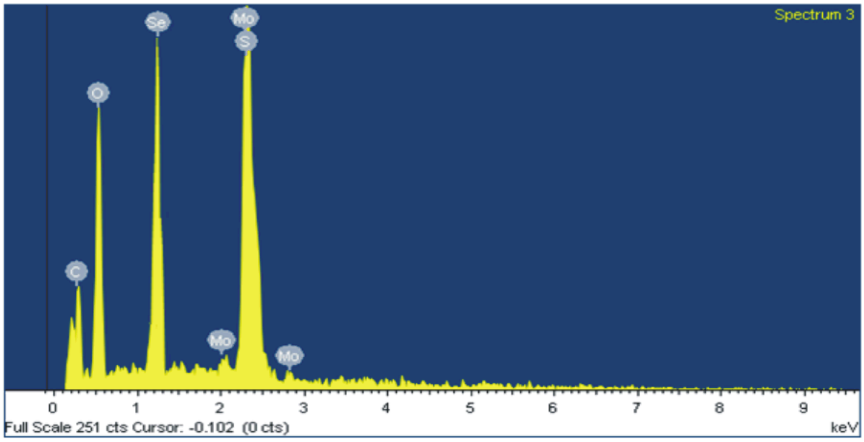

Fig. 6: EDX spectrum of electrodeposited MoSSe thin films

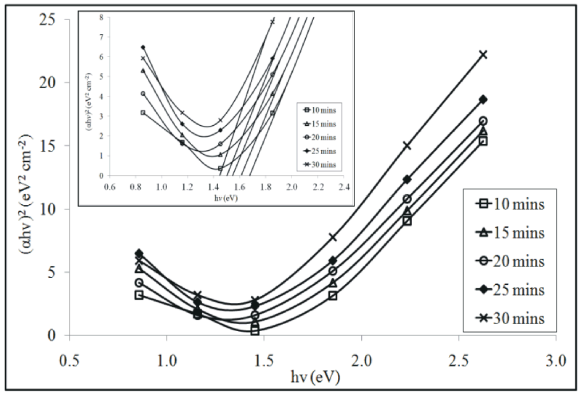

Fig. 7: hv vs. (ahv) 2 plots of MoSSe thin films coated at different deposition times

hydrous films. Unsymmetrical crystallites due the separation and precipitation of sulphide and selenide phases in ternary chalcogenide films are also observed on the surface of the films [19].

This main advantage of EDX is it possesses the capability for the detection of low atomic number elements such as carbon and oxygen, which are ubiquitous in our environment [20]. Figure 6 shows the EDX patterns for electrodeposited ternary MoSSe thin film deposited at 30 minutes.

Referring to the spectra, strong peaks for Mo, S and Se were identified. The overlapping peaks for Mo and S elements has been identified as a limitation of the EDX technique due to the corresponding X-rays generated by the emission from different energy-level shells (K, L and M). Although elements C and O do not play any role in the synthesis of the films, their peaks can be observed in the spectrum. Furthermore, an inclusion of oxygen is observed for all the films because it is found to be unavoidable for chemically deposited films as testified [21-22]. This is true and accepted for all films synthesized.

Optical Properties of Electrodeposited Thin Films: From the optical transmittance spectrum obtained, the corresponding bandgap energy of the thin films was studied via analysis of the Tauc plot of the films [23]. The nature of the bandgap and its value can be calculated using this Tauc plot. Figure 7 presents Tauc plot of MoSSe thin films deposited at different deposition times (see inset graph).

The resulting plot has a distinct linear regime which denotes the onset of absorption and extrapolation. This linear region to the abscissa yields the energy of the optical band gap of the material. A prominent feature that can be seen in the hν vs. $(\acute{a}h\nu)^2$ plots is that the linear portion of the plot energy is greater than 2 eV. This is an indication of a direct transition type of material [24]. Hence, a graph of $h\nu$ vs. $(\acute{a}h\nu)^2$ is drawn and the optical bandgap energy has been estimated by extrapolating the straight line portion to cut the energy axis. It is noticed that the E_g decreased from 1.66 eV to 1.44 eV with the increase of deposition time of the films, which are in good range with the reported value for ternary molybdenum sulphoselenide thin films prepared by arrested precipitation technique (APT) [19]. The corresponding values of the bandgap energy of the films with respect to film thickness are given in Table 2.

According to the results on the optical properties of MoSSe thin films, it can be concluded that the optical bandgap energy of all type of films decreases as the deposition time of the film increases. This results correlates to film thickness, whereby an increase in deposition time of the films results in a greater thickness. When the deposition conditions like substrate

Table 2: Bandgap energy values corresponding to film thickness of MoSSe thin films

Deposition Time (mins)	Film Thickness (ìm)	Bandgap (eV)
10	0.8423	1.66
15	0.9142	1.61
20	0.9923	1.54
25	1.0673	1.50
30	1.1582	1.44

temperature of the film and solution concentration are kept fixed, the value of the band gap in general changes according to the thickness. The reason is due to the changing barrier height because of the variation in grain size in the polycrystalline film. The reason that we consider this effect is that a decrease in barrier height is caused by an increase in grain size which in turn caused by an increase in film thickness. A decrease with an increase in thickness in direct band gap is also observed by Dheepa *et al*. [25].

Semiconductor Parameters of Electrodeposited Thin Films: A tabulation of the potential-capacitance behaviour data of MoSSe thin films for the system n-MoSSe | polyiodide | graphite electrode is done by plotting the inverse of the square of the capacitance versus the applied potential to the films. In the Mott-Schottky graphs of $1/C^2$ sc versus V_{SCE}, the voltage axis intercepts give the flat band potentials V_{FB}. The slopes of the straight line portions of the Mott-Schottky plots can be used to determine the charge carrier concentration, N.

The tabulation is a Mott-Schottky plot, which is obtained for MoSSe films. In terms of experimental voltages, the Mott Schottky equation is defined as:

$$\frac{1}{C^2} = \frac{2\left(V - V_{FB} - k_B T / e\right)}{e e_0 \, e \, N} \tag{5}$$

Where C is the space charge capacitance, k_B is the Boltzmann's constant (1.38 x 10G^{23} J/K), T is the temperature of the operation (300 K), e is the electronic charge (1.603 x 10G^{19} C), , is the dielectric constant of MoSSe, $,_o$ is the dielectric constant of free space (8.854 x 10G^{12} F / m) and N is the carrier concentration which is calculated from the slope of the graph.

The dielectric constants, , for the films have been evaluated by using the relation:

$$e = \frac{Cd}{A \, e_0} \tag{6}$$

Where C is the capacitance, *d* is the thickness of the crystal and A is the area of contact. Another important parameter to be deduced is the depletion layer width (W) and the band bending (V_b) that can be calculated from the relation:

$$V_b = V_{F,redox} - V_{FB}$$
$$W = \left(\frac{2 e e_0 \, V_b}{e \, N} \right)^{1/2} \tag{7}$$

Where V_b is the built in voltage or the band bending and $V_{F,redox}$ is the redox potential of the $2I^- / I_2$ redox couple equal to 0.295 V_{SCE}(Chandra *et al*. 1984). An expression for the density of states, N_c can be written as:

$$N_c = \frac{2}{h^3}\left(2p \, m_e^* \, kT\right)^{3/2} \tag{8}$$

Where *h* is the Planck's constant (4.136 x 10G^{15} eV s) m_e is the effective electron mass in the conduction band and taken as . 0.5 m_e for molybdenum chalcogenides [26].

The semiconductor parameters of ternary molybdenum chalcogenide MoSSe thin films by Mott-Schottky plot for at different deposition time are shown in Figure 8.

The linear portions of the plots are extrapolated to the potential axis in order to determine the flatband potential (V_{FB}) of the films. The results of the flatband potential and semiconductor parameters are shown in Table 3.

It is observed that the semiconductor parameter values for MoSSe are intermediate between the reported values for $MoSe_2$ and MoS_2 [9, 10, 27]. This trend is in agreement with Gujarathi *et al.* (2006) whereby they reported intermediate values for WS_xSe_{2-x} from the end members of the series WS_xSe_{2-x} (i.e. WSe_2 and WS_2) [1].

The positive slope of the plot in Figure 8 confirms the n-type material. The flat band potential (V_{FB}) value was observed to decrease from -0.29 to -0.38 *V* as the deposition time increased. This is due to increase in crystallinity of the films in thicker films. The decreasing values for the depletion width of the films are in good agreement with the energy gap values retrieved from optical studies. The dielectric constants for the films are also observed to decrease in thicker films. The dielectric constant value determined the capability of objects of a given size, such as sets of metal plates, to hold their electric charge for long periods of time and/or to hold large quantities of charge. Although the dielectric constant for MoSSe thin films decreases with time, this is

Table 3: The Mott-Schottky plots for MoSSe films

	MoSSe thin film				
Semiconductor parameters	10 mins	15 mins	20 mins	25 mins	30 mins
Type of semiconductor	n	n	n	n	n
Flat band potential (V_{FB}) (V)	-0.29	-0.30	-0.33	-0.36	-0.38
Dielectric constant (ɡ)	41	32.4	30.5	29.5	30.1
Doping density (N)× 10^{29} (mɢ^3)	1.65	1.09	0.84	0.68	0.57
Depletion layer width (W) (Å)	3.96	3.16	2.51	1.95	1.61
Density of states in Conduction Band (N_c)× 10^{13} (mɢ^3)	4.196	4.196	4.196	4.196	4.196
Band bending (V_b) (V)	0.585	0.595	0.625	0.655	0.675
Energy gap (E_g) (eV)	1.66	1.61	1.54	1.50	1.44

a good trend because a higher dielectric constant is not necessarily desirable. Generally, substances with high dielectric constants break down more easily when subjected to intense electric fields, than do materials with low dielectric constants. Hence, the values obtained from the Mott-Schottky plots are accepted with good agreements with the reports given.

CONCLUSION

Results proved that ITO-coated glass and stainless steel substrates were used to deposit the ternary MoSSe thin films. All films obtained were well adherent to the substrates with an 'ion-by-ion' growth mechanism. XRD analysis of the films proved polycrystalline MoSSe thin films with rhombohedral structure. Their lattice parameters are estimated as a = b = 0.9533 nm and c = 1.7363 nm. EDX pattern confirmed that mixed combinatorial films of MoSSe have been formed through the electrodeposition process. The grain size in the films was found to be dependent on thickness and a decrease in the direct optical bandgap transition energy of the film was observed. Results on the semiconductor parameters of the films revealed it is of n-type material and all semiconductor values come in the range of a semiconductor films which can be suitable for photo electrochemical solar cells as tomorrow's energy needs are greatly going to utilized with solar energy.

ACKNOWLEDGEMENT

The work presented in this manuscript was supported by the Ministry of Higher Education (MoHE), sponsored by KeTTHA/FRGS grant (Project No. FRGS/ 2011/ FKP/ TK02/ 1 F00120) and Universiti Teknikal Malaysia Melaka (UTeM).

REFERENCES

1. Gujarathi, D.N., G.K. Solanki, M.P. Deshpande and M.K. Agarwal, 2006. PEC behaviour of mixed single crystals of tungsten sulphoselenide grown by a CVT technique, Solar Energy Materials and Solar Cells, 90(16): 2630-2639.
2. Anand, T.J.S. and K. Senthil, 2007. Capacitance-Voltage studies on soft selenized $MoSe_2$ films for PEC cells, IEICE Technical Report. Electron Devices, 107(2): 277-280.
3. Anand, T.J.S., 2009. Synthesis and Characterization of MoS_2 Films for Photoelectro- chemical Cells, Sains Malaysiana, 38(1): 85-89.
4. Patel, M. and A. Roy, 2012. Enhancement of output performance of Cu_2ZnSnS_4 thin film solar cells - A numerical simulation approach and comparison to experiments, Physica B, 407(21): 4391-4397.
5. Sun, S., Z. Zou and G. Min, 2009. Synthesis of tungsten disulfide nanotubes from different precursor, Materials Chemistry and Physics, 114(2/3): 884-888.
6. Srivastava, S.K. and D. Patil, 2005. Defect studies by X-ray diffraction, electrical and optical properties of layer type tungsten mixed molybdenum sulphoselenide, Solid State Ionics, 176(5/6): 513-521.
7. Calva, E.B., M.O. Lopez, A.A. Garcia and Y.M. Kwabara, Optical properties of silver sulphide thin films formed on evaporated Ag by a simple sulphurization method, Thin Solid Films, 518(7): 1835-1838.
8. Ghosh, S.K., T. Bera, O. Karacasu, A. Swarnakar, J.G. Buijnsters and J.P. Celis, 2011. Nanostructured MoS_x - based thin films obtained by electrochemical reduction, Electrochimica Acta, 56(5): 2433-2442.

9. Pouzet, J., H. Hadouda, J.C. Bernede and R. Leny, 1996. MoS_2 thin films obtained by a new technique: Solid state reaction between the constituents in thin film form, Journal of Physics and Chemistry of Solids, 57(9): 1363-1369.
10. Anand, T.J., S.C. Sanjeeviraja and M. Jayachandran, 2001. Preparation of layered semiconductor ($MoSe_2$) by electrosynthesis, Vacuum, 60(4): 431-435.
11. Zainal, Z., N. Saravanan and H.L. Mien, 2005. Electrodeposition of nickel selenide thin films in the presence of triethanolamine as a complexing agent, Journal of Materials Science and Materials Electrononics, 16(2): 111-117.
12. Anuar, K., W.T. Tan, M.S. Atan, K. Dzulkefly, S.M. Ho, H. Md Jelas and N. Saravanan, 2007. Cyclic Voltammetry Study of Copper Tin Sulfide Compounds, Pacific Journal of Science and Technolology, 8(2): 252-260.
13. JCPDS, ICDD, Card No. 1-71-6685.
14. Hankare, P.P., V.M. Bhuse, K.M. Garadkar, S.D. Delekar and I.S. Mulla, 2003. Low temperature route to grow polycrystalline cadmium selenide and mercury selenide thin films, Materials Chemistry and Physics, 82(3): 711-717.
15. Baumes, L.A., M. Moliner and A. Corma, 2009. Design of a Full-Profile-Matching Solution for High-Throughput Analysis of Multiphase Samples through Powder X-ray Diffraction, Chemistry-European Journal, 15(8): 4258-4269.
16. JCPDS, ICDD, Card No. 33-397.
17. Kale, R.B. and C.D. Lokhande, 2005. Systematic study on structural phase behavior of CdSe thin films, Journal of Physics and Chemistry B, 109(43): 20288-20294.
18. Abdullah, H., N. Saadah and S. Shaari, 2012. Effect of deposition time on ZnS thin films properties by chemical bath deposition (CBD) technique, World Applied Sciences Journal, 19(8): 1087-1091.
19. Ajalkar, B.D., R.K. Mane, B.D. Sarwade and P.N. Bhosale, 2004. Optical and electrical studies on molybdenum sulphoselenide [Mo $(S_{1-x}Se_x)_2$] thin films prepared by arrested precipitation technique (APT), Solar Energy Materials and Solar Cells, 81(1): 101-112.
20. Herguth, W.R. and G.W. Nadeau, 2011. Particle characterization and sizing: SEM utilizing automated electron beam and AFA software for particle counting and particle characterization, Journal of ASTM. International, 8: JAI103381.
21. Lokhande, C.D., B.R. Sankapal, R.S. Mane, H.M. Pathan, M. Muller, M. Giersig and V. Ganesan, 2002. XRD, SEM, AFM, HRTEM, EDAX and RBS studies of chemically deposited Sb_2S_3 and Sb_2Se_3 thin films, Applied Surface Science,193(1/4): 1-10.
22. Naik, R., S.K. Parida, C. Kumar, R. Ganesan and K.S. Sangunni, 2012. Optical properties change in $Sb_{40}S_{40}Se_{20}$ thin films by light-induced effect, Journal of Alloys and Compounds, 522(5): 172-177.
23. Murphy, A.B., 2007. Band-gap determination from diffuse reflectance measurements of semiconductor films and application to photoelectrochemical water-splitting, Solar Energy Materials and Solar Cells, 91(14): 1326-1337.
24. Kokate, A.V., M.R. Asabe, S.D. Delekar, L.V. Gavali, I.S. Mulla, P.P. Hankare and B.K. Chougule, 2006. Photoelectrochemical properties of electrochemically deposited $CdIn_2S_4$ thin films, Journal of Physics and Chemistry of Solids, 67(11): 2331-2336.
25. Dheepa, J., R. Sathyamoorthy and A. Subbarayan, 2005. Optical properties of thermally evaporated Bi_2Te_3 thin films, Journal of Crystal Growth, 274(1/2): 100-105.
26. Chandra, S., D.P. Singh, P.C. Srivastava and S.N. Sahu, 1984. Electrodeposited semiconducting molybdenum selenide films: II. Optical, electrical, electrochemical and photoelectrochemical solar cell studies, Journal of Physics D: Applied Physics, 17(4): 2125-2138.
27. Shariza, S. and T.J.S. Anand, 2011. Effect of Deposition Time on the Structural and Optical Properties of Molybdenum Chalcogenides Thin Films, Chalcogenide Letters, 8(9): 529-539.